Dear Author,

Here are the proofs of your article.

- You can submit your corrections **online**, via **e-mail** or by **fax**.
- For **online** submission please insert your corrections in the online correction form. Always indicate the line number to which the correction refers.
- You can also insert your corrections in the proof PDF and **email** the annotated PDF.
- For fax submission, please ensure that your corrections are clearly legible. Use a fine black pen and write the correction in the margin, not too close to the edge of the page.
- Remember to note the **journal title**, **article number**, and **your name** when sending your response via e-mail or fax.
- **Check** the metadata sheet to make sure that the header information, especially author names and the corresponding affiliations are correctly shown.
- **Check** the questions that may have arisen during copy editing and insert your answers/ corrections.
- **Check** that the text is complete and that all figures, tables and their legends are included. Also check the accuracy of special characters, equations, and electronic supplementary material if applicable. If necessary refer to the *Edited manuscript*.
- The publication of inaccurate data such as dosages and units can have serious consequences. Please take particular care that all such details are correct.
- Please **do not** make changes that involve only matters of style. We have generally introduced forms that follow the journal's style.
  Substantial changes in content, e.g., new results, corrected values, title and authorship are not allowed without the approval of the responsible editor. In such a case, please contact the Editorial Office and return his/her consent together with the proof.
- If we do not receive your corrections **within 48 hours**, we will send you a reminder.
- Your article will be published **Online First** approximately one week after receipt of your corrected proofs. This is the **official first publication** citable with the DOI. **Further changes are, therefore, not possible.**
- The **printed version** will follow in a forthcoming issue.

Please note

After online publication, subscribers (personal/institutional) to this journal will have access to the complete article via the DOI using the URL: http://dx.doi.org/[DOI].
If you would like to know when your article has been published online, take advantage of our free alert service. For registration and further information go to: http://www.link.springer.com.

Due to the electronic nature of the procedure, the manuscript and the original figures will only be returned to you on special request. When you return your corrections, please inform us if you would like to have these documents returned.

Metadata of the article that will be visualized in OnlineFirst

ArticleTitle	Synthesis and Characterization of Aluminophosphates Type-5 and 36 Doubly Modified with Si and Zn and Its Catalytic Application in the Reaction of Methanol to Hydrocarbons (MTH)	
Article Sub-Title		
Article CopyRight	Springer Science+Business Media, LLC, part of Springer Nature (This will be the copyright line in the final PDF)	
Journal Name	Topics in Catalysis	
Corresponding Author	Family Name	**Ruiz**
	Particle	
	Given Name	**Misael García**
	Suffix	
	Division	Doctorado en Ciencia de Materiales de La Facultad de Química
	Organization	Universidad Autónoma del Estado de México
	Address	Paseo Colón Esquina Paseo Tollocan S/N, C.P. 50000, Toluca Estado de México, Mexico
	Phone	
	Fax	
	Email	misagr89@gmail.com
	URL	
	ORCID	
Author	Family Name	**Casados**
	Particle	
	Given Name	**Dora A. Solís**
	Suffix	
	Division	
	Organization	Universidad Autónoma del Estado de México, Centro Conjunto de Investigación en Química Sustentable UAEM-UNAM, Personal Académico Adscrito a La Facultad de Química, UAEMex
	Address	Toluca, Mexico
	Phone	
	Fax	
	Email	
	URL	
	ORCID	
Author	Family Name	**Pliego**
	Particle	
	Given Name	**Julia Aguilar**
	Suffix	
	Division	
	Organization	Área de Química Aplicada, Departamento de Ciencias Básicas, UAM-A
	Address	San pablo 180, C.P. 02200, Mexico, Mexico
	Phone	

	Fax	
	Email	
	URL	
	ORCID	
Author	Family Name	**Álvarez**
	Particle	
	Given Name	**Carlos Márquez**
	Suffix	
	Division	
	Organization	Instituto de Catálisis Y Petroleoquímica, CSIC
	Address	C/Marie Curie 2, Campus Cantoblanco, 28049, Madrid, Spain
	Phone	
	Fax	
	Email	
	URL	
	ORCID	
Author	Family Name	**Andrés**
	Particle	**de**
	Given Name	**Enrique Sastre**
	Suffix	
	Division	
	Organization	Instituto de Catálisis Y Petroleoquímica, CSIC
	Address	C/Marie Curie 2, Campus Cantoblanco, 28049, Madrid, Spain
	Phone	
	Fax	
	Email	
	URL	
	ORCID	
Author	Family Name	**Tartalo**
	Particle	
	Given Name	**Diana Sanjurjo**
	Suffix	
	Division	
	Organization	Instituto de Catálisis Y Petroleoquímica, CSIC
	Address	C/Marie Curie 2, Campus Cantoblanco, 28049, Madrid, Spain
	Phone	
	Fax	
	Email	
	URL	
	ORCID	
Author	Family Name	**Sanchez-Sanchez**
	Particle	
	Given Name	**Manuel**
	Suffix	
	Division	

	Organization	Instituto de Catálisis Y Petroleoquímica, CSIC
	Address	C/Marie Curie 2, Campus Cantoblanco, 28049, Madrid, Spain
	Phone	
	Fax	
	Email	
	URL	
	ORCID	
Author	Family Name	**Casas**
	Particle	
	Given Name	**Marisol Grande**
	Suffix	
	Division	
	Organization	Instituto de Catálisis Y Petroleoquímica, CSIC
	Address	C/Marie Curie 2, Campus Cantoblanco, 28049, Madrid, Spain
	Phone	
	Fax	
	Email	
	URL	
	ORCID	

Schedule	Received	
	Revised	
	Accepted	

Abstract	This paper presents a study of the synthesis of $AlPO_4$-5 and $AlPO_4$-36 materials doubly substituted by Si and Zn, as acid function and aromatizing function, respectively. The physicochemical properties of the zeotypes were studied by XRD, adsorption of N_2, Temperature Programmed Desorption with NH_3, ^{31}P MAS NMR and SEM. The incorporation of Zn and Si has shown an important effect on the acidic, textural and morphological properties of the samples. The particle size has a significant effect on the catalytic activity in the reaction of methanol to hydrocarbons in terms of methanol conversion and selectivity. It was observed that as the particle size decreases, the methanol conversion increases causing the catalyst to deactivate in a shorter time. The incorporation of Zn improved the selectivity to total aromatics by the aromatizing effect of Zn. The SAPO-5 (S5) material having a smaller particle size showed complete conversions of methanol. In contrast, the ZnAPO-5 (Z5) material showed low conversions but a high selectivity to total aromatics (41%). On the other hand, the material S36-2 presented a high selectivity to aromatics (58%) due to the high amount of Zn and Si. Both metals provided a certain acidic character to the materials.

Keywords (separated by '-')	Methanol conversion - Zeotypes - Aromatics - BTX fraction - AlPO doubly substituted - MeAPSO materials

Footnote Information	**Electronic supplementary material** The online version of this article (https://doi.org/10.1007/s11244-020-01266-3) contains supplementary material, which is available to authorized users.

Topics in Catalysis
https://doi.org/10.1007/s11244-020-01266-3

ORIGINAL PAPER

Synthesis and Characterization of Aluminophosphates Type-5 and 36 Doubly Modified with Si and Zn and Its Catalytic Application in the Reaction of Methanol to Hydrocarbons (MTH)

Misael García Ruiz[1] · Dora A. Solís Casados[2] · Julia Aguilar Pliego[3] · Carlos Márquez Álvarez[4] · Enrique Sastre de Andrés[4] · Diana Sanjurjo Tartalo[4] · Manuel Sanchez-Sanchez[4] · Marisol Grande Casas[4]

Abstract

This paper presents a study of the synthesis of $AlPO_4$-5 and $AlPO_4$-36 materials doubly substituted by Si and Zn, as acid function and aromatizing function, respectively. The physicochemical properties of the zeotypes were studied by XRD, adsorption of N_2, Temperature Programmed Desorption with NH_3, ^{31}P MAS NMR and SEM. The incorporation of Zn and Si has shown an important effect on the acidic, textural and morphological properties of the samples. The particle size has a significant effect on the catalytic activity in the reaction of methanol to hydrocarbons in terms of methanol conversion and selectivity. It was observed that as the particle size decreases, the methanol conversion increases causing the catalyst to deactivate in a shorter time. The incorporation of Zn improved the selectivity to total aromatics by the aromatizing effect of Zn. The SAPO-5 (S5) material having a smaller particle size showed complete conversions of methanol. In contrast, the ZnAPO-5 (Z5) material showed low conversions but a high selectivity to total aromatics (41%). On the other hand, the material S36-2 presented a high selectivity to aromatics (58%) due to the high amount of Zn and Si. Both metals provided a certain acidic character to the materials.

Keywords Methanol conversion · Zeotypes · Aromatics · BTX fraction · AlPO doubly substituted · MeAPSO materials

Abbreviations

MTH	Methanol to hydrocarbons
MTA	Methanol to aromatics
MTO	Methanol to olefins
$AlPO_4$-n	Microporous crystalline aluminophosphate
MeAPO	Microporous crystalline aluminophosphate containing a transition metal ion
MeAPSO	Microporous crystalline aluminophosphate doubly substituted by two transition metal iones
BTX	Bencene, toluene and xilenes fraction
AFI	Aluminophosphate five structure
TRI	Tridymite structure
ATS	Aluminophosphate thirty-six structure
MCHA	*N*-Methyldicyclohexylamine
TPA	Tripropylamine
WHSV	Weight hourly space velocity
SEM	Scanning electron microscopy
ICP-OES	Inductively coupled plasma optical emission spectrometry
NMR	Nuclear magnetic resonance
BET	Brunauer–Emmett–Teller equation
SM	Substitution isomorphic
XRD	X-ray diffraction
TPD	Temperature programmed desorption

Electronic supplementary material The online version of this article (https://doi.org/10.1007/s11244-020-01266-3) contains supplementary material, which is available to authorized users.

✉ Misael García Ruiz
misagr89@gmail.com

[1] Doctorado en Ciencia de Materiales de La Facultad de Química, Universidad Autónoma del Estado de México, Paseo Colón Esquina Paseo Tollocan S/N, C.P. 50000 Toluca Estado de México, Mexico

[2] Universidad Autónoma del Estado de México, Centro Conjunto de Investigación en Química Sustentable UAEM-UNAM, Personal Académico Adscrito a La Facultad de Química, UAEMex, Toluca, Mexico

[3] Área de Química Aplicada, Departamento de Ciencias Básicas, UAM-A, San pablo 180, C.P. 02200 Mexico, Mexico

[4] Instituto de Catálisis Y Petroleoquímica, CSIC, C/Marie Curie 2, Campus Cantoblanco, 28049 Madrid, Spain

TGA	Thermogravimetric analyses
DTG	Derivate thermogravimetric
SDA	Structure-directing agent
MR	Member rings

1 Introduction

Methanol can be produced via syngas from multifarious carbon resources such as coal, natural gas and biomass, the conversion of methanol to hydrocarbons (MTH) over acidic zeolite catalysts has studied as into an increasingly important alternative to petroleum processing to get various fuel and chemical products [1]. The conversion of methanol to hydrocarbons (MTH) over acidic zeolites has drawn considerable attention since its discovery in 1970s by Mobil Corporation [2]. Depending on the product of reaction selectivity, this process was named as MTG (methanol to gasoline), MTO (methanol to olefins), MTP (methanol to propene) and MTA (methanol to aromatics). In this last process, aromatic compounds, especially benzene, toluene and xylene (BTX fraction) are mainly produced from the oil-based route to this date, the gradual depletion of oil reserves has resulted in a sustained tight supply and high cost of aromatics [3]. However, methanol can be expediently produced via syngas from multifarious carbon resources such as coal, natural gas and biomass [4]. The MTH chemistry and its commercial potential have been known for decades. In the late 1970s, New Zealand build the world's first facility for producing gasoline from natural gas via methanol using synthetic zeolites called ZSM-5 [2]. Several authors been studied HZSM-5 zeolite as a catalyst for MTH reaction because of its shape selectivity, high activity, and excellent hydrothermal stability [5].

Aluminophosphates (AlPOs), first reported by Wilson in 1982 [6], constitute a large class of molecular sieves or zeotypes. Zeotypes are extensively investigated and applied in the field of catalysis because of their intrinsic properties such as high micropore areas, narrow micropore distribution, high thermal stability and capacity of being doped by different heteroatom ions, which generate heterogeneous active sites within structures with shape-selective ability [7]. These materials not only exhibit characteristics of zeolites but also show novel physicochemical properties that are linked to their unique composition and have potential applications in catalysis, adsorption, and ion-exchange [8].

Isomorphic substitution of framework Al^{3+} and P^{5+} ions by metal cations (V, Co, Mg, Ga, Fe, Zn, etc.) or silicon produces the MeAPO and SAPO family materials, respectively. The incorporation of cations can lead to Brønsted acid sites, which make these materials useful in acid-catalyzed reactions [9, 10]. This acid property of SAPO is strongly dependent on the Si content, sitting and ordering in the lattice. When Si atoms are incorporated into the framework of an $AlPO_4$ at the phosphorous sites (mechanism SM2), a potential Bronsted site per Si atom would be generated. Simultaneous replacement of a pair of Al + P atoms by two Si atoms (mechanism SM3 in combination with mechanism SM2), according to the model SM3 + SM2 proposed by Dwyer et al. [11] thus creating silicon islands. Depending on the relative rates of the SM3 and SM2 mechanisms, the size and terminating environment of the Si islands vary. when the SM2 mechanism dominates, the silicon islands grow to smaller sizes terminating with a $Si(OAl)_4$ environment that render the edge a negative charge which can host a proton, thus forming a Brønsted acid site [12]. Regarding zinc, taking into account its oxidation state, zinc is expected to be incorporated into the framework by the SM1 replacement mechanism (occupying an aluminum position).

On the other hand, there are other materials denominated MeAPSO, where Zn and Si are incorporated, replacing Al and P, respectively. These materials were studied in the present work where it is proposed that Zn acts as aromatizing agent and Si as an acidic agent. These materials were evaluated in the reaction of methanol to hydrocarbons (MTH).

MeAPSO materials can be considered potential catalysts for the MTA reaction, due to the presence of Zn and Si in the structure. In this study, the catalytic activity of two types of structures named MeAPSO-5 (AFI) and MeAPSO-36 (ATS) are compared. We will work with structures with channels of 12 members with large pores such as $AlPO_4$-5 or $AlPO_4$-36.

In this context the P or Al atoms of the network can easily be replaced by Si or Zn, respectively, generating acidity. In the present work, the aim is the synthesis of doubly substituted AlPOs, by Zn as aromatizing function and Si as an acid function. The amount of silicon and zinc incorporated in the materials was varied systematically, so that the composition of the synthesis gels can be directly related to the properties of the materials obtained. It is important to note that these types of materials have not been studied in the MTH process previously.

2 Experimental

2.1 Materials

The reagents used for the preparation of zeolites are tetraethyl orthosilicate (TEOS, 98%, Aldrich), aluminum hydroxide hydrated ($Al(OH)_3$, Sigma-Aldrich), zinc acetate dihydrate ($Zn(CH_3COO)_2$ $2H_2O$, 99% Sigma Aldrich), tripropylamine (TPA, 99%, Aldrich), N-methyldicyclohexylamine (MCHA, 99%, Aldrich), Phosphoric acid (H_3PO_4, 85 wt% in H_2O, Aldrich).

Journal : Large 11244 | Article No : 1266 | Pages : 14 | MS Code : 1266 | Dispatch : 20-4-2020

2.2 Synthesis of MeAPSO-36 Materials

MeAPSO-36 was synthesized according to the reported procedure [10]. The gels were prepared using phosphoric acid (H_3PO_4, 85% in water, Aldrich), Hydrated aluminum hydroxide ($Al(OH)_3$-xH_2O, Aldrich) and tripropylamine (TPA, 99%, Aldrich) with a composition of 1.0 P: y Zn: 1-y Al: x Si: 0.8 TPA:10 H_2O.

In a typical synthesis H_3PO_4 and $Al(OH)_3$-xH_2O were dissolved in deionized H_2O under continue stirring for 15 min. Upon dissolution, zinc diacetate ($Zn(CH_3$-$COO)_2$-$2H_2O$) was slowly added to the solution under vigorous stirring until a homogeneous gel was achieved. Finally, the SDA was added to the gel dropwise and then rapidly with vigorous stirring by 1 h. Gels were then placed in Teflon (PTFE) lined stainless steel autoclaves and heated for 18 h at 160 °C. Then products were filtered, washed with distilled water, and dried at 100 °C for one night. As-prepared samples were calcined at 550 °C for 6 h under an air flow. Previously, the sample has been heating with a rate of 1 °C/min under a N_2 flow and maintained for 1 h at 550 °C under this atmosphere.

First, the molar ratio of zinc (y) was modified between 0 and 0.15, keeping the amount of silicon constant in the gels (x). Complementarily in a second stage, the amount of zinc that was incorporated in the synthesis gels (y = 0.1) was kept constant and the silicon content (x) of them was modified between 0 and 0.25. The gel composition and synthesis conditions are presented in Table 1.

2.3 Synthesis of MeAPSO-5 Materials

MeAPSO-5 samples were synthesized by hydrothermal treatment using N-methyldicyclohexylamine (MCHA) as SDA according to the reported procedure [13]. The gel composition was 1.0 P: y Zn: 1-y Al: x Si: 0.8 MCHA: 25 H_2O. The molar composition of the reaction mixtures and the synthesis conditions for the different MeAPSO-5 materials obtained are given in Table 4. Samples were synthetized over similar condition to MeAPSO-36, however the synthesis temperature was 175 °C and 4 h. Finally, the samples were calcined under the same conditions mentioned previously. The gel composition and synthesis conditions are presented in Table 2.

2.4 Catalyst Characterization

Powder X-ray diffraction (PXRD) patterns were collected with an XPert Pro PANalytical diffractometer (CuKα1 radiation = 0.15406 nm). Scanning electron microscopy (SEM) images were recorded on a Hitachi S-3000 N microscope. Transmission electron microscopy (TEM) study was carried on a JEOL 2100F microscope opering to 200 kV. Nitrogen adsorption/desorption isotherms were measured at − 196 °C in a Micromeritics ASAP 2020 device. Before the measurement, the previously calcined sample was degassed at 350 °C under high vacuum for at least 10 h. Surface areas were estimated by the BET method whereas microporous and external surface areas were estimated by applying the t-plot method.

Table 1 Synthesis of SAPO-5. Molar composition of gel: 1.0 P: y Zn: 1-y Al: x Si: 0.8 MCHA: 25 H_2O

Sample	Denoted	Amount of Zn in moles (y)	Amount of Si in moles (x)	Product phase
A5-0.02 Zn-0.15 Si	S5-1	0.02	0.15	AFI + TRI
A5-0.05 Zn-0.02 Si	S5-2	0.05	0.02	AFI + TRI
A5-0.05 Zn-0.05 Si	S5-3	0.05	0.05	AFI + TRI
A5-0.15 Zn-0.15 Si	S5-4	0.15	0.15	AFI + TRI
A5-0.15 Si (SAPO-5)	S5	–	0.15	AFI
A5-0.04 Zn (ZnAPO-5)	Z5	0.04	–	AFI

Table 2 Synthesis of SAPO-36

Sample	Denoted	Amount of Zn in moles (y)	Amount of Si in moles (x)	Product pase
A36-0.01 Zn (ZnAPO-36)	Z36	0.01	–	ATS
A36-0.05 Zn-0.15 Si	S36-1	0.05	0.15	ATS + AFI
A36-0.1 Zn-0.05 Si	S36-2	0.1	0.05	ATS + AFI
A36-0.1 Zn-0.15 Si	S36-3	0.1	0.15	ATS + AFI
A36-0.1 Zn-0.25 Si	S36-4	0.1	0.25	ATS + AFI
A36-0.15 Zn-0.15 Si	S36-5	0.15	0.15	ATS

Molar composition of gel: 1.0 P: y Zn: 1-y Al: x Si: 0.9 TPA:10 H_2O

Journal : Large 11244 | Article No : 1266 | Pages : 14 | MS Code : 1266 | Dispatch : 20-4-2020

Solid-state magic-angle spinning (MAS) NMR experiments were conducted on a Bruker Avance 300 (11.75 T) spectrometer operated with frequency at 130.32 MHz and spinning rate at 10 kHz. The 27Al NMR spectra were recorded using a pulse width of 0.5 μs (π/12 flip angle), 2400 scans and a recycle delay of 1 s.

The Al, Si, P and Zn concentrations of samples were obtained by inductively coupled plasma-optical emission spectroscopy (ICP-OES) with a Optima 3300 DV Perkin Elmer. Temperature programmed desorption of ammonia (NH_3-TPD) was conducted using a Micrometrics Autochem II chemisorption analysis equipment. Typically, 100 mg of sample pellets (30–40 mesh) were pretreated at 550 °C for 1 h in helium flow (25 mL/min) and then cooled to the adsorption temperature (177 °C). A gas mixture of 5.0 vol% NH_3 in He was then allowed to flow over the sample for 4 h at a rate of 15 mL/min. Afterwards, the sample was flushed with a 25 mL/min helium flow for 30 min while maintaining the temperature at 177 °C to remove weakly adsorbed NH_3, and finally the temperature was increased to 550 °C at a rate of 10 °C/min. Thermogravimetric analysis (TGA) were carried out at a heating of 30 °C to 900 °C with a rate of 20 °C/min under air flow and registered in a PerkinElmer TGA7 instrument.

2.5 MTH Catalytic Testing Conditions

Zeotypes materials were tested as catalysts in the conversion of methanol at 400 °C in a Microactivity reaction set (PID Eng & Tech) consisting of a fixed bed reactor completely automated and controlled from a computer. The reactor outlet is connected to a gas chromatograph to analyze the reaction products. N_2 was used as a stripping gas under a controlled flow. The methanol was fed as a liquid using an HPLC pump (Gilson 307). The methanol was converted to the gas phase and mixed with the N_2 stream in a preheater at 180 °C to generate a gas mixture with a constant molar ratio of methanol/N_2 of 4. Before the reaction, the catalysts were activated at 550 °C for 1 h low air flow to remove any trace of organic molecules or moisture adsorbed within the pores of the catalyst. The weight of the catalyst (sieved in a 20–30 mesh, corresponding to a particle size between 0.84 and 0.59 mm) and the flow of methanol were optimized to achieve different values of space velocities (WHSV).

The reaction products were analyzed online by gas chromatography with a VARIAN CP3800 chromatograph. The device is equipped with two columns: (i) a Petrocol DH50.2 capillary column connected to an FID detector, and (ii) a HayesepQ packed column (2 m length, 3.17 mm (1/8″) diameter external and 2 mm internal diameter) connected to a TCD detector, to analyze hydrocarbons and oxygenated products, respectively.

3 Results and Discussion

3.1 X-Ray Diffraction

The XRD pattern of the substituted MeAPSO-36 material with different amounts of Si and Zn are show in Fig. 1a. In all the samples, the peaks position and the intensities are identical to those reported for SAPO-36 [14], however, there are minor differences in the XRD patterns in each sample depending on the Zn and Si content of the samples. ATS structure is favored by the presence of zinc in the structure of MeAPSO-36, as well as low silicon content and high synthesis temperature, the S36-5 XRD pattern contains only ATS-type structure, due to the high amount of moles of Zn present in the sample. Wilson et al. [6] reported that the synthesis of MeAPO-36 the high concentration of metals

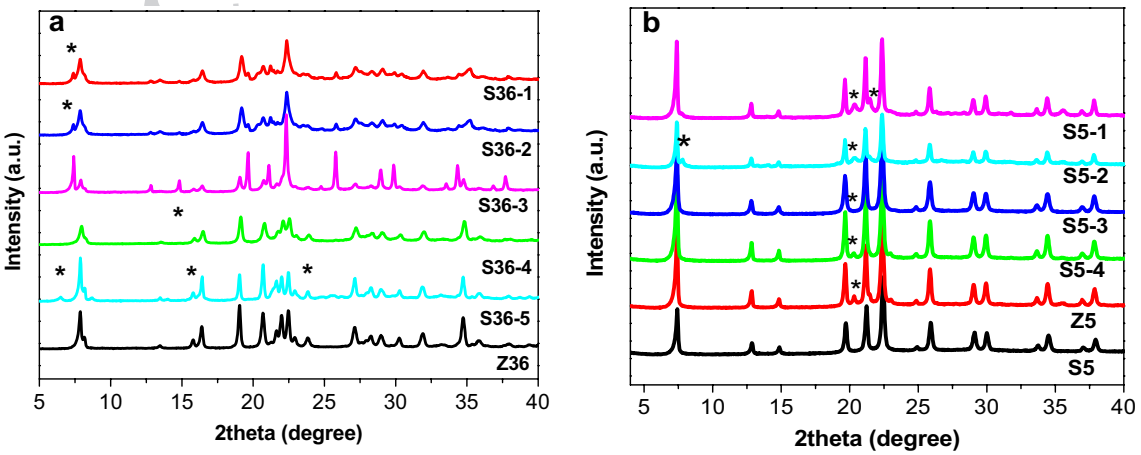

Fig. 1 XRD patterns of **a** MeAPSO-36 and **b** MeAPSO-5 materials synthetized

Journal : Large 11244 | Article No : 1266 | Pages : 14 | MS Code : 1266 | Dispatch : 20-4-2020

such as zinc favors the crystallization of the MeAPSO-36 over that of its competitive co-phase structure type 5 (AFI). It is observed that as the amount of Zn increases in the peak samples corresponding to the AFI structure (marked with asterisks) it disappears, which indicates that the stability of the crystalline structure increased with the Zn content. Sample S36-4 has a low Zn content and a high Si content, so it showed an increase in the appearance of co-phase structure AFI.

For the other hand, the XRD patterns of the MeAPSO-5 samples are show in Fig. 1b, S5 (SAPO-5) material shows a pattern of AFI structure without any impurity. In particular, the use of MCHA as the SDA for synthesis SAPO-5 samples, can forming AFI structure without any additional impurity phases. The other samples showed a small amount of impurity identified as the tridymite phase [15] coexisting with the AFI-type structure. The impurity phase was also observed by Chen et al. [16] when loading a higher amount of metal onto the AFI framework of $AlPO_4$-5. As high amount zinc the intensity of those diffraction peaks attributed to tridymite and berlinite significantly increase. The ratio of 0.9 mol of SDA is enough to form an $AlPO_4$-5 phase. It is known that AFI structure increases with an increase of pH or the SDA content [17].

3.2 *N_2 Adsorption–Desorption*

All as-prepared MeAPSO samples were studied by N_2 adsorption/desorption isotherms at 77 K in order to determine their textural properties. Isotherms of MeAPSO-5 and MeAPSO-36 samples are showed in Fig. S1a and S1b (material supplementary 1a and 1b), respectively. All the samples present type I isotherms (according to the IUPAC classification [18]), corresponding to microporous materials. The steep uptake at low relative pressures in MeAPSO-36 samples is due to adsorbent-adsorptive interactions in narrow micropores and the subsequent formation of a monolayer (Fig. S1a). The shape of the isotherm at higher relative pressures (up to p/po = 1) is due to unrestricted monolayer-multilayer adsorption. At higher relative pressures, the N_2 adsorption–desorption curve of MeAPSO-36 samples exhibits hysteresis H4-type, which is characteristic of molecular sieves with formation of inter or intracrystalline mesopores as will be observed by SEM analysis later [19, 20].

Figure S1b presents the N_2 adsorption–desorption isotherm of MeAPSO-5 samples. Similarly, the N_2 adsorption capacity of all materials is high at low relative pressures, indicating the presence of a microporous structure with an H4-type hysteresis loop formed almost throughout the P/Po range although to a lesser extent compared to the MeAPSO-36 samples [21, 22]. It may be considered that.

MCHA structure-directing agent constrained in the unidimensional 12-ring pore channels generated larger pores, giving mesoporous $AlPO_4$-5 [22].

The micropore volumes and BET areas for the samples prepared using different silicon and zinc contents are summarized in Table 3. It can be observed that all the samples have surface area in the range 550–650 m^2/g for MeAPSO-5 materials. However, the MeAPSO-36 materials presented smaller areas in the range 200 and 320 m^2/g. These differences can be explained in base to the longer crystal size and the higher intercrystalline porosity in MeAPSO-36 materials in addition show very low non-microporous (external) surface, values characteristic of this type of materials. High

Table 3 Elemental composition measured by ICP-OES and NMR ^{31}P and textural properties of the samples

Catalyst	% wt				P/Zn ratio (ICP)[a]	P/Zn ratio (NMR)[b]	S_{BET} (m^2/g)	S_{micro} (m^2/g)[c]
	% Al	% P	% Zn	% Si				
S5-1	16.2	23.7	1.4	2.4	34.3	–	268.6	264.4
S5-2	21.6	19.2	2.5	0.4	16.3	8.3	176.5	114.5
S5-3	17.7	22.4	2.2	0.5	21.9	10.2	198.4	104.8
S5-4	7.7	18.9	3.3	2.7	11.9	11.4	148.2	55.6
S5	19.4	18.3	–	4.7	–	–	300.5	174.6
Z5	12.3	27.2	5.1	–	11.1	11.6	140.9	71.8
Z36	14.3	26.8	6.9	–	8.1	6.8	124.2	110.5
S36-1	11.6	21.1	2.9	3.6	15.4	11.3	326.5	249.4
S36-2	12.4	21.4	6.4	1.2	7.1	6.4	164.2	139.7
S36-3	17.1	22.2	7.3	0.7	6.4	4.6	153.7	120.2
S36-4	12.8	26.9	6.9	2.8	8.2	8.0	175.6	129.6
S36-5	13.9	20.8	6.5	2.8	6.7	6.5	74.7	13.8

[a]P/Mg ration derived from chemical analysis

[b]P/Mg ration of original samples derived from ^{31}P-MAS NMR using dmfit program for convolution process

[c]Using t-plot method

Journal : Large 11244 | Article No : 1266 | Pages : 14 | MS Code : 1266 | Dispatch : 20-4-2020

silicon content led to a distinct decrease of BET surface area and microporous volume due to the existence of amorphous SiO_2 [23], however, our obtained BET surface area of SAPO-5 materials are larger than the literature reported values 286 m^2/g and [22]. This is mainly caused by the higher external surface areas, which may be attributed to mesopore formation. Therefore, the coexistence of micropores and mesopores in our sample leads to high BET surface area.

3.3 Scanning Electron Microscopy (SEM)

Figures S2 and S3 (material supplementary) show SEM selected images of MeAPSO-36 and MeAPSO-5, respectively. The amount of Si and Zn had influences in a considerate way distribution of crystals sizes and shapes of MeAPSO materials. MeAPSO-36 materials selected (samples Z36, S36-1, S36-2 and S36-4 in Table 1) presented crystals particles with irregular spheres larger of size 16–22 µm range (Figure S2) formed in turn by small crystals in the form of thin needles [8]. In this study, the crystal size decreased in the order Z36 > S36-1 > S36-4 > S36-2 which is also in agreement with the observed relative stability. The intercrystalline space of these crystals is the cause of the formation of an H4 hysteresis cycle visualized in the N_2 isotherms.

Figure S3 shows SEM pictures for the MeAPSO-5 materials selected. Solid only silicon content (S5) presented homogeneous distribution of spherical particles, which have a diameter of ca. 1.5 µm. Sample Z5 (only zinc content) consists of homogeneously distributed large porous spherical particles with an approximate diameter of ca. 15 µm [20]. S5.1 presented the same size of particles. However, the S5-2 material presented a different morphology, particles in the form of 3D hexagons with approximately 10 µm sizes are observed, this can be attributed to a higher content of Zn (0.15 mol) incorporated in the material. In this study, the crystal size decreased in the order S5 > Z5 > S5-1 > S5-2.

3.4 TGA y DTG Analysis

Thermogravimetric analyses (TGA) were performed aiming to verify the incorporation of the SDA molecules in the structure of the as-made samples and their subsequent complete elimination after and before calcination. The TGA/DTG curves of selected material MeAPSO-36 y MeAPSO-5 not calcined selected are shown in Fig. 2a, b, respectively. TGA profiles are strongly influenced by the Zn and Si incorporation. In both figures, three weight losses are observed. The first weight loss, at temperatures below 150 °C (step I), can be attributed to desorption of adsorbed water. The second weight loss, between 400 and 550 °C (step II) is due to the decomposition of the template in each case (TPA and MCHA) and, finally, the third weight loss at temperatures higher than 600 °C (step III) has been associated with the further removal of organic residues occluded in the channels and cages of the MeAPSO materials caused by combustion [24]. The rest of the TGA/DTG curves of the MeAPSO-5 and MeAPSO-36 materials are shown in the complementary material S4a and S4b, respectively.

It can be observed that the decomposition of the template occurs in a different way for sample S36-3. The fact that the template decomposition began at lower temperature in this sample could be possibly attributed to its smaller particle size and the lesser diffusional problems derived from it. On the other hand, in Figures S5 (supplementary material S5) presented the curves TGA and DTG, of some MeAPSO-36 and MeAPSO-5 selected after calcining. In all cases, a single loss of mass less than 100 °C is observed, which corresponds to the physisorption of water retained in the samples. No

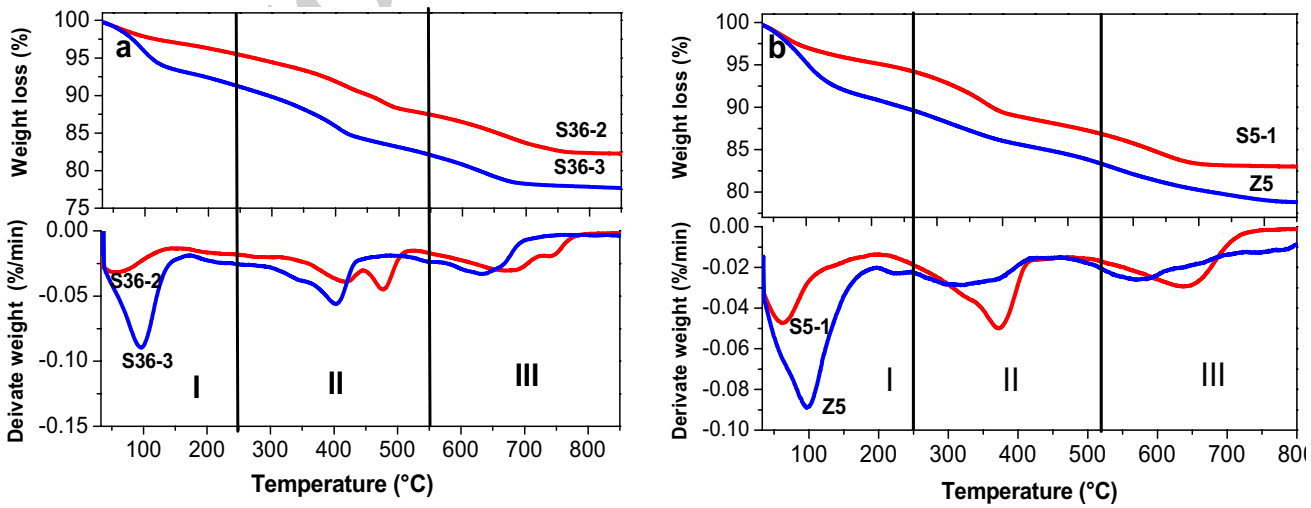

Fig. 2 Thermal analysis of the MeAPSO uncalcined materials selected TGA (top) and DTG (bottom) **a** MeAPSO-36 and **b** MeAPSO-5 selected

Journal : Large 11244 | Article No : 1266 | Pages : 14 | MS Code : 1266 | Dispatch : 20-4-2020

other significant weight losses are observed at higher temperature which indicates that the SDA was eliminated.

3.5 ICP-OES Chemical Composition Analysis

The elemental compositions of the molecular sieves are presented in Table 3. The content of Al, P, Si and Zn was determined, the correct incorporation of zinc and silicon is verified, as already mentioned above, zinc is incorporated according to the substitution mechanism SM1 (occupying an aluminum position), while silicon can be incorporated isolated occupying a phosphorus position or in pairs replacing a pair Al + P (mechanisms SM2 and SM3 respectively). With these values, the P/Zn molar ratio was determined and compared with that calculated by ^{31}P NMR spectrum using Eq. 1 reported by Barrie and Klinowski [25].

$$\mathrm{P/Zn} = \sum_{n=0}^{4} I_p(nAl) / \sum_{n=0}^{4} 0.25(4-n) I_P(nAl) \quad (1)$$

where Ip(nAl) being the area of the peak due to the P (n Al, 4-n Zn) structural units calculated by ^{31}P MAS NMR shows later. The value of Ip was calculated using the spectrum convolution process using the dmfit program created by Massiot et al. [26].

3.6 *Solid State NMR Spectroscopy of ^{31}P MAS*

The incorporation of Zn to the MeAPSO framework was studied by ^{31}P MAS NMR. The ^{31}P spectrum of MeAPSO-36 and MeAPSO-5 materials are showed in Fig. 3a, b, respectably. The ^{31}P resonance peak is asymmetrically broadened, which points out a wide distribution of phosphorous sites with different chemical environment [25]. It has been described that when the amount of zinc incorporated to the MeAPSO-5 framework (Fig. 3a) is low, P atoms are located in a unique P(4Al) environment resulting from the substitution of phosphorous by silicon in the aluminophosphate framework (in their second coordination sphere) [27, 28] as case of S5 (SAPO-5). However, if the zinc content is higher (S5-4), multiple phosphorous environments can occur. The ^{31}P spectrum has a peak at 28 ppm (attributed to P(4A1) sites) and a broad shoulder at 23 ppm indicative of phosphorus having a neighbor other than aluminum, i.e. P(3A1, 1Zn) site in the ATS framework [14, 25].

Similarly, the ^{31}P spectrum of MeAPSO-36 materials (Fig. 3b) presented the signal at 28 ppm attributed to the P (4Al) sites [29], followed by a shoulder at 23 ppm (3 Al, 1 Zn) and another signal in the case of material S36-5 (higher content of Zn) at 18 ppm corresponding to 2 Zn as neighbors of the phosphorous denoted as P(2 Al, 2 Zn) [14].

The P/Zn ratio of the materials determined by chemical analysis and ^{31}P NMR spectrum are showed in Table 3. The difference observed between both values indicates that a significant amount of Zn is not occupying the framework sites [30]. This technique is a useful tool to demonstrate the correct incorporation of Zn, because the coordination of P is sensitive to the incorporation in the second sphere of coordination by Zn measured by NMR. However, in materials with low zinc content, such as S5-1, only the signal belonging to P (4Al) is observed, so Eq. 1 cannot be applied.

3.7 *Temperature-Programmed Desorption (NH_3-TPD)*

The acidity of the calcined samples has been evaluated by TPD-NH_3. TPD profiles of the MeAPSO-36 and MeAPSO-5 samples are showed in Fig. 4a, b, respectably. In principle, the increase in the molar ratio of zinc and silicon in gels

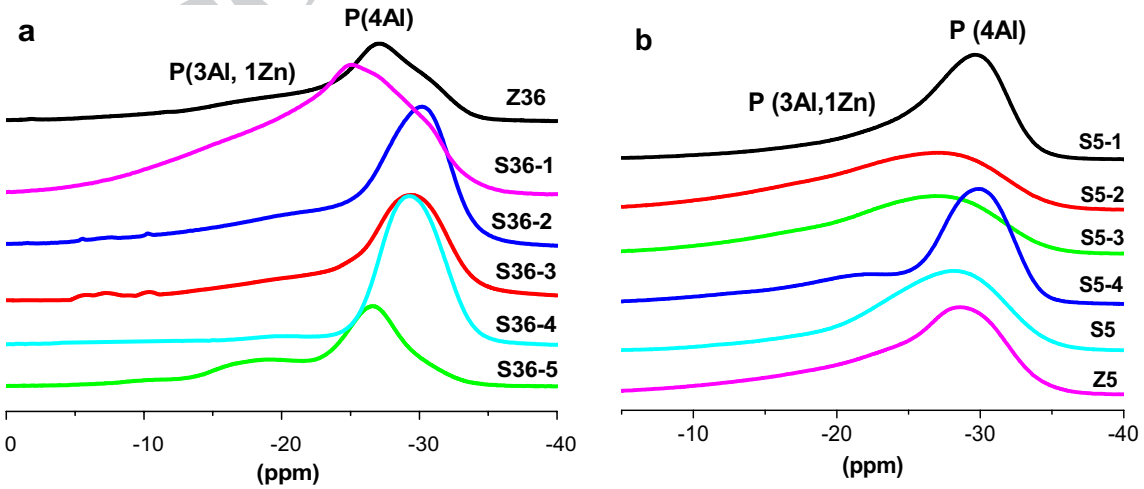

Fig. 3. ^{31}P MAS NMR spectra of double modified $AlPO_4$ materials **a** MeAPSO-36 and **b** MeAPSO-5

Journal : Large 11244 | Article No : 1266 | Pages : 14 | MS Code : 1266 | Dispatch : 20-4-2020

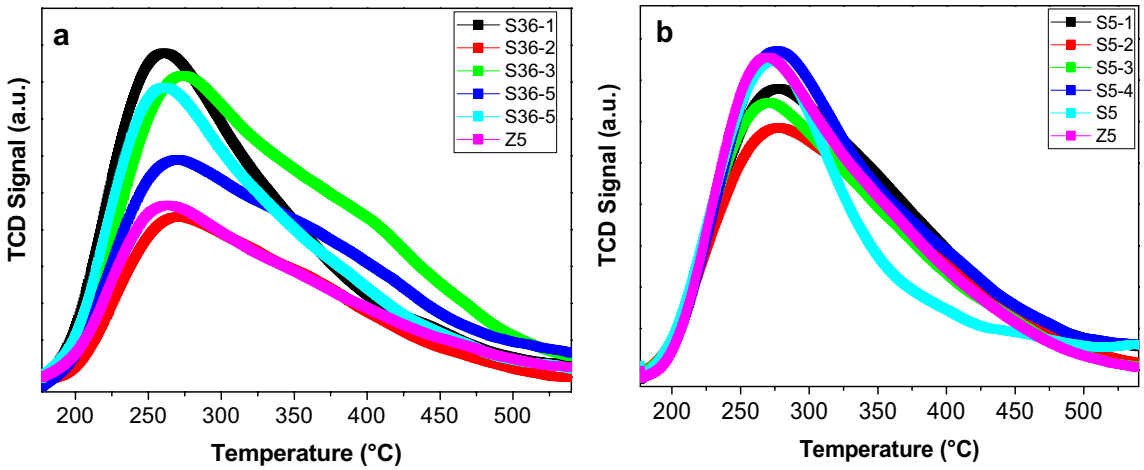

Fig. 4 TPD-NH_3 profiles of double modified $AlPO_4$ materials **a** MeAPSO-36 and **b** MeAPSO-5

implies a greater incorporation of both metals in solids, which causes a greater density of weak acid sites. It can be observed that all samples show a maximum at around 270 °C, indicating that these acid sites are relatively weak characteristic of this type of materials. This signal could be tentatively assigned to desorption of ammonia on Brønsted acid sites originated by isomorphic substitution of Al^{3+} by Zn^{2+} and P^{4+} by Si^{3+} in the MeAPSO structures [31, 32]. However, it is well known that this technique does not allow distinguishing between Brönsted and Lewis acid sites. Therefore, it cannot be excluded that some Lewis acid centres able to adsorb ammonia at moderate temperature are present in the MeAPSO material, probably formed during the calcination treatment [33]. MeAPSO samples with different zinc and silica content show slightly different TPD profiles. The incorporation of zinc species in MeAPSO materials exhibits a significant influence on the distribution of acid sites, when the amount of Zn is increased and if the density of acidic sites increases, it is intuited that the substitution of both metals in the structure provides certain acidic character to the materials, especially for samples S5-4 and S36-5, which have high amounts of substituted Si. The acid property of MeAPSO materials is strongly dependent on the Si content, sitting and ordering in the lattice. SM2 substitution leads to more acid centers while SM2 + SM3 combination lead to less acid centers but higher strength than the one arising from only the SM2 substitution [34].

The specific peak area is proportional to the number of acid sites in the sample and can be determined by integration by convolution of the area under the curve of the spectra. The amounts of strong and weak acid sites of the samples are listed in Table 4. The acids sites density total is higher in MeAPSO-5 samples indicating that MeAPSO-36 possesses weaker acid sites. These results indicate that the proportion of acid sites increased in the order S5 < Z5 < S5-2 < S5-1 < S5-3 < S5-4 for MeAPSO-5 materials and S36-2 < Z36 < S36-1 < S36-5 < S36-4 < S36-3 for MeAPSO-36 materials. It has been shown that substitution of both metals can alter the acid sites properties of materials and therefore is led to change in selectivity of catalysts to different products.

Table 4 Acidity properties of materials

Catalyst	Temperature (°C)	Acidity (μmol NH_3/g) Weak acid (LT)
S5-1	280	273.45
S5-2	277	261.85
S5-3	272	325.41
S5-4	273	337.18
S5	274	144.83
Z5	277	191.93
Z36	271	151.63
S36-1	263	230.93
S36-2	275	149.56
S36-3	272	312.91
S36-4	268	291.12
S36-5	261	259.78

3.8 Catalytic Evaluation

3.8.1 Catalytic Evaluation of MeAPSO-5

A range of catalytic studies have been few undertaken to establish the performance of these metal doubly substituted systems. However, from a catalytic point of view, topologies with 1D pore systems (as MeAPSO materials) possess inherent drawbacks when compared with the 3D ones (zeolites), due to both the diffusional problems of chemicals and the quicker deactivation of the catalysts found in the former [35,

Journal : Large 11244 | Article No : 1266 | Pages : 14 | MS Code : 1266 | Dispatch : 20-4-2020

36]. As demonstrated by some authors where they report the activity of zeolites in the MTO and MTA reactions using ZSM-5 catalysts [37, 38]. They reported the high activity due to the 3D topology of zeolitic materials with high selectivities to aromatics compared to zeotype materials. Furthermore, the particle size is a strongly important factor for improving the catalyst life like the acid density; the decrease in the crystallite size leads to the increase in the catalyst life [39].

Figure 5 shows the methanol conversion of MeAPSO-5 materials under conditions of a space velocity (WHSV) 4.24/h, 400 °C and 0.5 g of catalyst. Among the different parameters that influence the stability of these catalysts, especially the particle size and the acid strength of the active centres have been considered the most important factors affecting the deactivation during the reaction. The S5 material (only silicon, aluminum and phosphorus) showed higher conversion levels during the 9 h reaction due presented a smaller particle size (1.5 µm) and by the generation of Bronsted type acid sites due to the combination of SM2 + SM3 mechanisms. The Z5 material (constituted of zinc, aluminum and phosphorus) showed very minor methanol conversions compared to the other catalysts, due it had a larger particle size (20 µm diameter), which causes rapid deactivation. Some authors mentioned [40, 41] that particle size and acid properties of the catalyst have influence on catalyst lifetime in MTH reaction. In general, a smaller particle size improves the diffusion efficiency and accessibility of acid sites for high catalytic activity obtaining higher methanol conversion values [42, 43].

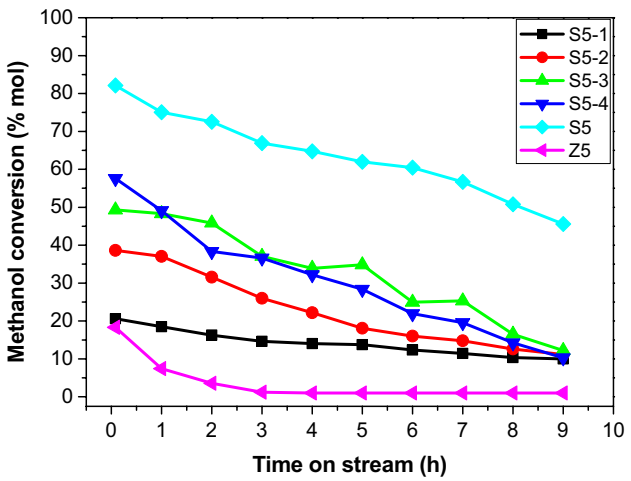

Fig. 5 Results of methanol conversion in MTH reaction over MeAPSO-5 catalyst Conditions reaction: WHSV of 4.24/h, 400 °C, 0.5 g of catalyst

Table 5 shows distribution of reaction products of MeAPSO-5 materials at short reaction times (TOS 5 min) and 400 °C with similar conversion values It is observed that as the amount of Zn increases, the selectivity increases to total aromatics and therefore the BTX fraction, stating the aromatizing effect of Zn when it is incorporated by isomorphic substitution. All the catalysts showed a selectivity to olefins close to 50% mol, which may be related with acid properties of the materials (weak acid).

In the MTH reaction, the product distribution is strongly dependent on the acid strength of zeotype catalysts. In particular, the S5-1 material presented a low aromatic selectivity (26.9%) due a low zinc amount, however, the selectivity to olefins was high (49.6%). These results were with a low methanol conversion value (18%) at 5 min of reaction, this can be associated with a large particle size measured by SEM. these materials have a selectivity to light olefins (ethylene and propylene) around 50% in all cases, which may indicate that Si can provide acidity necessary to form olefins as mentioned by some authors. SAPO-5 catalyst used above has the 12-ring pores with 0.73 nm straight channels and more alkane molecules can be adsorbed and react with acid centers in SAPO-5 channels due to its large channels and more pore-mouth exposed [44]. The Z5 material composed of Zn, Al and P had the highest selectivity to total aromatics and therefore to BTX selectivity, due to the high content of the aromatizing agent. The total aromatic selectivity increased in the following order, with respect to the table shown: Z5 > S5-1 > S5-2. As mentioned above, these types of materials have not been studied in the MTH reaction, however, materials of the SAPO-5 type have been studied by some authors. Terasaka et al. [45] synthesized SAPO-5 samples with different morphologies and sizes and they demonstrated the high catalytic activity of the SAPO-5 exclusively in the MTO process. They demonstrated the high catalytic activity of the SAPO-5 exclusively in the MTO

Table 5 Distribution of reaction products of MeAPSO-5 catalysts in the similar conversion of methanol level

Sample	% Methanol conversion	Selectivity (%mol)			Particule size SEM (µm)
		Olefins	Total aromatics	BTX fraction	
S5-1	20.5	49.6	26.9	2.2	20
S5-2	38.6	53.6	16.0	2.1	10
Z5	18.3	33.9	41.0	2.0	20

Reaction conditions: TOS 5 min, WHSV 4.24/h, 400 °C, 0.5 g catalyst

process with complete methanol conversions and selectivity to light olefins (C2 to C4) c.a. 60%.

3.8.2 Catalytic Evaluation of MeAPSO-36

Figure 6 shows the methanol conversion of MeAPSO-36 materials with a spatial velocity (WHSV) 2.12/h, 400 °C and 1 g of catalyst. The deactivation process of the MeAPSO-36 catalysts is slower than the MeAPSO-5 catalysts, resulting in conversion curves vs reaction time up to 25 min due to smaller channels and acidity. The deactivation of the catalyst was thus ascribed to the formation of the bulky aromatic coke in the structure [46]. The fast deactivation could be explained by the shorter size ring in $AlPO_4$-36 materials (7.4 × 6.5 Å) that favor of the formation of bulkier organic compounds that cause deactivation. Additionally, it is observed that again the particle size (measured by SEM) had a significant influence on the conversion of methanol. The material S36-3 (green line) has higher conversion levels, generating a complete conversion of methanol at 5 min of reaction reaching deactivation after 25 min of reaction. On the contrary, the sample S36-4 (blue line) showed the lowest conversion level at 5 min (40% mol) reaching deactivation at 10 min, should be attributed to the larger particle size of this catalyst (20 µm). Additionally, the lower methanol conversion over this material is because of the partial transformation of the active catalyst (ATS) phase to less active phase (tridymite).

Regarding the distribution of reaction products, Table 6 shows the catalytic activity of MeAPSO-36 materials. Similarly, all the catalysts produced aromatics compounds as the main-product followed by olefins, at the expense of the S36-1 material due to the low amount of zinc (0.05 Zn mol) a large particle size (20 µm). Selectivity to total aromatics is related to the amount of Zn incorporated into the structure and to the particle size, a higher molar concentration of Zn, greater selectivity to aromatics and therefore greater selectivity to the BTX fraction. Specifically, the material Z36 (MeAPO-36) presented a high selectivity to aromatics due to aromatizing effect of Zn. On the other hand, S36-2 material presented a total aromatic selectivity of 46.3%, this is due to the fact that it has the high amount of Zn and 0.05 mol of Si, providing both an acidic (Si) effect and a Zn aromatizing effect isomorphic substitution.

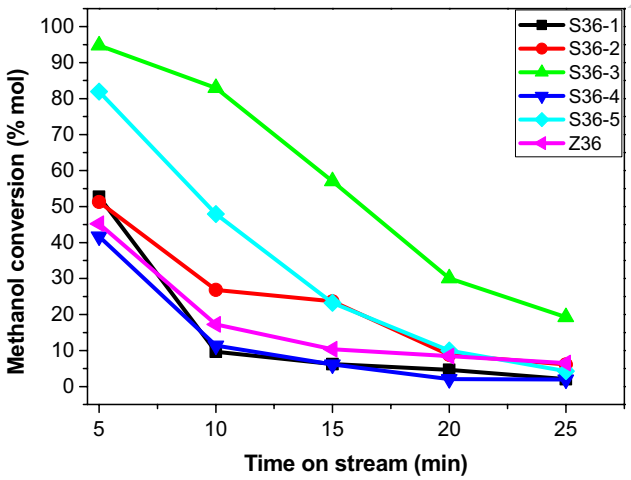

Fig. 6 Results of methanol conversion in MTH reaction over MeAPSO-36 catalyst Conditions reaction: WHSV of 2.12/h, 400 °C, 1 g of catalyst

3.8.3 Distribution of Reaction Products for MeAPSO-5 Materials

Selectivities to the different type of products detected in the effluent stream as a function of time are showed in Fig. 7 for MeAPSO-5 materials tests carried out at WHSV = 4.24/h and 400 °C. The formation of aromatics (top) and light olefins (bottom) increases with time on stream in most cases. Sample S5-4 presented selectivities greater than total aromatics (blue line) with a value of approximately 60% at 9 h of reaction, which could be attributed to the presence of high amounts of Zn and Si and the high acidity generated for both metals.

The selectivity to light olefins remains constant during the 9 h of reaction even at low conversion rates, this could be ascribed to the growing blockage of the pores in the materials at low conversion rates, hindering the diffusion of the heavier reaction products and enhancing the release of less bulky hydrocarbons [46]. For example, material S5-3 was selective for light olefins (green line), due to low amounts of the aromatizing metal, followed by SAPO-5 material, which

Table 6 Distribution of reaction products of MeAPSO-36 catalysts in the similar conversion of methanol level

Sample	% Methanol conversión	Selectivity (% mol)			Particule size SEM (µm)
		Olefins	Total aromatics	BTX fraction	
Z36	40.4	36.2	57.2	4.25	20
S36-1	52.7	52.2	28.1	4.54	15
S36-2	51.8	42.9	46.3	2.07	15
S36-4	41.7	46.6	44.0	3.65	20

Reaction conditions: TOS 5 min, WHSV 2.12/h, 400 °C, 1 g catalyst

Journal : Large 11244 | Article No : 1266 | Pages : 14 | MS Code : 1266 | Dispatch : 20-4-2020

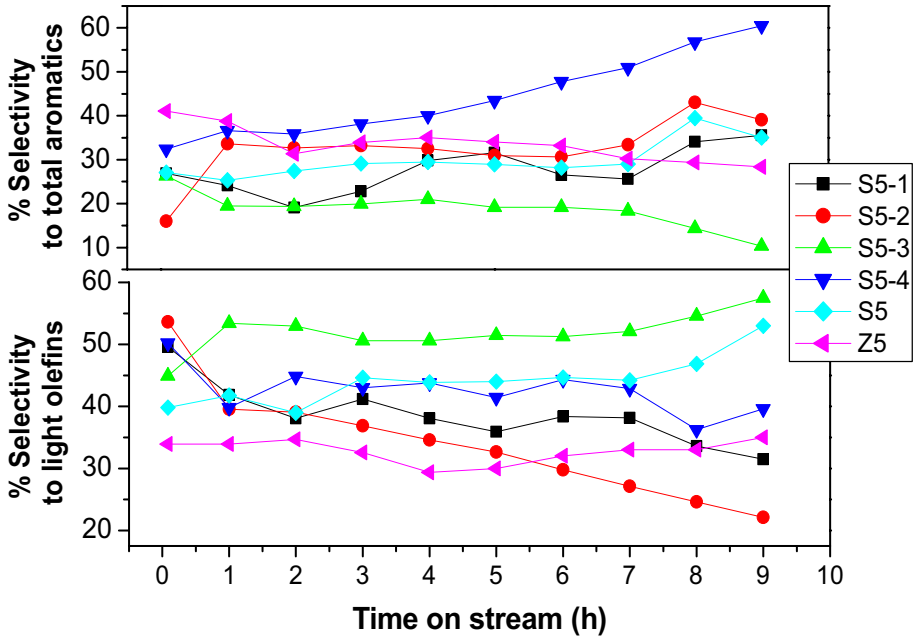

Fig. 7 % Selectivity to total aromatics (top) and % selectivity to light olefins (bottom) of MeAPSO-5 materials. Test conditions: T = 400 °C, WHSV = 4.24/h, 0.5 g of catalyst

is highly selective for olefins until 9 h reaction, as some authors report it [47]. These results could be attributed to the wider channels of MeAPSO-5 or might be also caused by a higher ratio of external acid sites, considering the higher microporous surface area of this material.

3.8.4 Distribution of Reaction Products for MeAPSO-36 Materials

Finally, selectivities to the different type of products of MeAPSO-36 are showed in Fig. 8 at WHSV = 2.12/h and 400 °C. It is notorious that the Z36 material is selective to the formation of aromatics (black line), because it is only composed of Zn, Al and P. Similar to MeAPSO-5 materials, it can be observed for all catalysts that the production of olefins and aromatics compounds is favored at low conversion

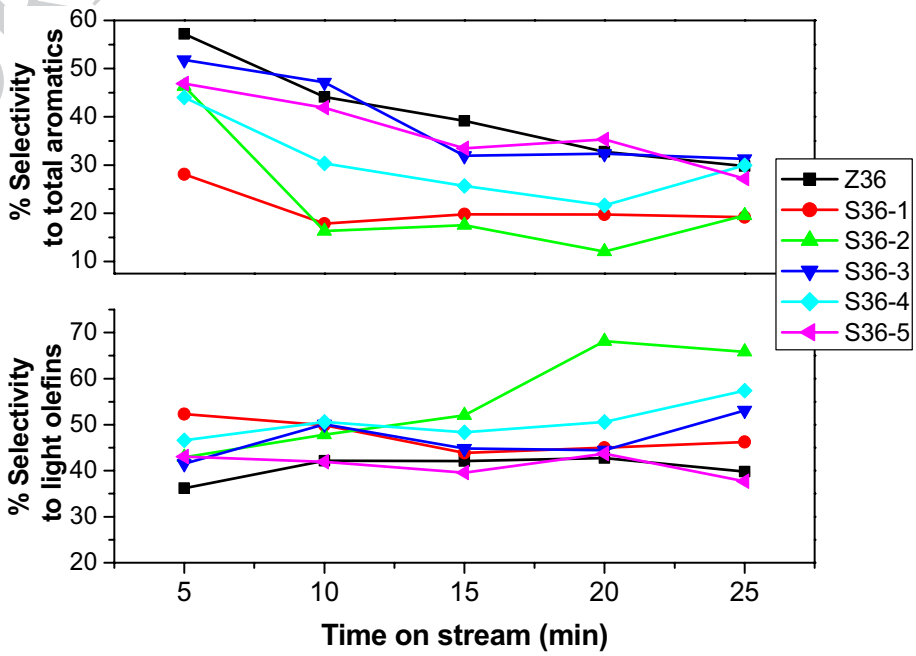

Fig. 8 % Selectivity to total aromatics (top) and % selectivity to light olefins (bottom) of MeAPSO-36 materials. Test conditions: T = 400 °C, WHSV = 1.12/h, 1 g of catalyst

rates. As discussed in the TPD-NH_3 analysis (Fig. 7b), the incorporation of Zn into the framework increases the density and strength of the acid sites. Thus, the increased density of active centers is more likely to influence the promotion of selectivity to aromatics compounds.

Regarding olefin selectivity, it is observed that the production of olefins remained constant during the reaction period except for sample S36-2 where olefin selectivity increased up to 60% after 15 min of reaction. The high activity of MeAPO-36 materials (Me^{2+}, Al and P) for obtaining aromatics has been previously studied by some authors [48]. However, doubly substituted materials have not been evaluated in this type of reaction. Finally, it was verified that the effects of acidity, particle size, pore structure, and crystal size of the zeotype, as well as effect of operation reaction conditions upon product selectivity.

4 Conclusions

Double-substituted $AlPO_4$-5 and $AlPO_4$-36 materials were synthesized with Si as an acid function and Zn as aromatizing function. The incorporation of Si and Zn by isomorphic substitution influenced the textural, as well as the morphology and catalytic performance of the zeotypes. The incorporation of Zn in MeAPSO-36 materials facilitated the formation of the ATS structure, since this structure is related to the incorporation of divalent metals such as Zn. TPD-NH_3 results further proved the incorporation of Si and Zn in the framework resulting in improved acidity and therefore had an influence on the catalytic activity for the formation of olefins and aromatic compounds.

The total aromatic selectivity increased as the amount of Zn in the MeAPSO materials increased, stating the aromatizing function of the divalent metal. The particle size had an important effect on the catalytic activity, as the particle size decreases, the methanol conversion increases causing the catalyst to deactivate in a shorter time. Specifically, the S5 material showed high conversions during the 9 h reaction when presenting a small particle size, however, the aromatic selectivity was lower because the material is only composed of Si, Al and P. Contrarily, the material represented a high selectivity to total aromatics at 5 min (41%) with low methanol conversions. Regarding the MeAPSO-36, the material S36-5 presented a high selectivity to aromatics due to the same amount of Zn and Si (0.15 mol). Both metals provided a certain acidic character to the materials. MeAPSO-36 suffered from fast deactivation because of the formation of coke favored by its shorter channels compared to MeAPSO-5 materials.

Acknowledgements The authors thank the Spanish Research Agency -AEI- and the European Regional Development Fund -FEDER- for the financing of this work, through the Project MAT2016-77496-R (AEI / FEDER, EU). MGR thanks the Molecular Sieve Group of the Institute of Catalysis and Petrochemistry (CSIC) in Madrid and CONACyT for the support granted for the research stay in Spain. I thank Dr. Massiot for the ease of having the admfit program and doing the NMR deconvolution process to make the necessary calculations.

Author Contributions All authors contributed to the study conception and design. Material preparation, data collection and analysis were performed by DASC (supervision), JAP (writing—review and editing), CMÁ (methodology), ESA (supervision), DST (investigation), MS-S and MGC (methodology). The first draft of the manuscript was written by PhD student, MGR and all authors commented on previous versions of the manuscript. All authors read and approved the final manuscript. We considerate the submitted is original and unique work and it has not been submitted to another journal simultaneity. The work is single study and it's not up into several parts and results are presented clearly, honestly, and without, falsification or inappropriate the data manipulation, the study submitted is part of my doctoral thesis.

Compliance with Ethical Standards

Conflict of interest The authors declare no conflict of interest. The funders had no role in the design of the study; in the collection, analyses, or interpretation of data; in the writing of the manuscript, or in the decision to publish the results.

Informed Consent Finally, additional informed consent was obtained from all individual participants for whom identifying information is included in this chapter.

Research Involving Human and Animal Rights This work does not contain any studies with human participants or animals performed by any of the authors.

References

1. Kianfar E, Hajimirzaee S, Mousavian S, Mehr AS (2020) Zeolite-based catalysts for methanol to gasoline process: a review. Microchem J 156:104822
2. Chang CD, Silvestri JA (1977) The conversion of methanol and other O-compounds to hydrocarbons over zeolite catalysts. J Catal 47:249–259
3. Zhang J, Qian W, Kong C, Wei F (2015) Increasing para-xylene selectivity in making aromatics from methanol with a surface-modified Zn/P/ZSM-5 catalyst. ACS Catal 5(5):2982–2988
4. Niu X, Gao J, Miao Q, Dong M, Wang G, Fan W, Qin Z, Wang J (2014) Influence of preparation method on the performance of Zn-containing HZSM-5 catalysts in methanol-to-aromatics. Microporous Mesoporous Mater 197:252–261
5. Bjørgen M, Svelle S, Joensen F, Nerlov J, Kolboe S, Bonino F, Palumbo L, Bordiga S, Olsbye U (2007) Conversion of methanol to hydrocarbons over zeolite H-ZSM-5: on the origin of the olefinic species. J Catal 249:195–207
6. Wilson ST, LokMessina BMCA, Cannan TR, Flanigen EM (1982) Aluminophosphate molecular sieves: a new class of microporous crystalline inorganic solids. JACS 104:1146–1147
7. Manjón-Sanz A, Sánchez-Sánchez M, Muñoz-Gómez P, García R, Sastre E (2010) Non-templated intercrystalline mesoporosity in heteroatom-doped $AlPO_4$-5 using N-methyldicyclohexylamine as structure-directing agent. Microporous Mesoporous Mater 131:331–341

Journal : Large 11244 | Article No : 1266 | Pages : 14 | MS Code : 1266 | Dispatch : 20-4-2020

8. Xu J, Zhou D, Song X, Chen L, Yu J, Ye C, Deng F (2008) Crystallization of magnesium substituted aluminophosphate of type-36 as studied by solid-state NMR spectroscopy. Microporous Mesoporous Mater 115:576–584
9. Kumar-Saha S, Waghmode SB, Maekawa H, Kawase R, Komura K, Kubota Y, Sugi Y (2005) Magnesioaluminophosphate molecular sieves with ATS topology: synthesis by dry-gel conversion method and catalytic properties in the isopropylation of biphenyl. Microporous Mesoporous Mater 81:277–287
10. O'Brien MG, Sanchez-Sanchez M, Beale AM, Lewis DW, Sankar G, Catlow CR (2007) Effect of organic templates on the kinetics and crystallization of microporous metal-substituted aluminophosphates. J Phys Chem C 111:16951–16961
11. Makarova M, Ojo A, Al-Ghefaili K, Dwyer J (1992) In: Proceedings of the IX international Zeolite conference, vol 2, p 259. Montreal, Canada
12. Gómez-Hortigüela L, Márquez-Álvarez C, Grande-Casas M, García R, Pérez-Pariente J (2009) Tailoring the acid strength of microporous silicoaluminophosphates through the use of mixtures of templates: control of the silicon incorporation mechanism. Microporous Mesoporous Mater 121:129–137
13. Sanchez-Sanchez M, Sankar G, Simperler A, Bell RG, Catlow CR, Thomas JM (2003) The extremely high specificity of N-methyldicyclohexylamine for the production of the large-pore microporous AFI material. Catal Lett 88(3–4):163–167
14. Prasad S, Dewey HB, Haw JF (1996) Probing acid sites in MAPO-36 by solid state NMR. Catal Lett 39:141–146
15. Graetsch HA (2002) Monoclinic $AlPO_4$ tridymite at 473 and 463 K from X-ray powder data. Acta Crystallogr C 58:18–20
16. Chen CM, Jehng JM (2004) Structure control of metal aluminum phosphate (MeAlPO-5) molecular sieves and applications in polyethylene glycol amination. Catal Lett 93(3–4):213–223
17. Du H, Fang M, Xu W, Meng X, Pang W (1997) Preparation by microwave irradiation of nanometre-sized AlPO4-5 molecular sieve. J Mater Chem 7:551
18. Thommes M, Kaneko K, Neimark A, Olivier J, Rodriguez-Reinoso F, Rouquerol J, Sing K (2015) Physisorption of gases, with special reference to the evaluation of surface area and pore size distribution (IUPAC Technical Report). Pure Appl Chem 87:1051–1069
19. Wang Q, Chen G, Xu S (2009) Hierarchical architecture observed in microspheres comprising microporous $AlPO_4$-11 nanocrystals. Microporous Mesoporous Mater 119:315–321
20. Basina G, Shamia DA, Polychronopoulou K, Tzitzios V, Balasubramanian VV, Dawaymeh F, Karanikolosa GN, Wahedi YA (2018) Hierarchical $AlPO_4$-5 and SAPO-5 microporous molecular sieves with mesoporous connectivity for water sorption applications. Surf Coat Tech 353:1–29
21. Gao B, Tian P, Li M, Yang M, Qiao Y, Wang L, Xu S, Liu Z (2015) In situ growth and assembly of microporous aluminophosphate nanosheets into ordered architectures at low temperature and their enhanced catalytic performance. J Mater Chem A 3:7741–7749
22. Utchariyajit K, Wongkasemjit S (2008) Structural aspects of mesoporous $AlPO_4$-5 (AFI) zeotype using microwave radiation and alumatrane precursor. Microporous Mesoporous Mater 114:175–184
23. Lin Y, Wei Y, Zhang L, Guo K, Wang M, Huang P, Meng X, Zhang R (2019) Facile ionothermal synthesis of SAPO-LTA zeotypes with high structural stability and their catalytic performance in MTO reaction. Microporous Mesoporous Mater 288:109611
24. Álvaro-Muñoz T, Márquez-Álvarez C, Sastre E (2012) Use of different templates on SAPO-34 synthesis: effect on the acidity and catalytic activity in the MTO reaction. Catal Today 179:27–34
25. Barrie PJ, Klinowski J (1989) Ordering in the framework of a magnesium aluminophosphate molecular sieve. J Phys Chem 93(16):5972–5974
26. Massiot D, Fayon F, Capron M, King I, Le Calvé S, Alonso B, Durand JO, Bujoli B, Gan Z, Hoatson G (2002) Modelling one- and two-dimensional solid state NMR spectra. Magn Reson Chem 40:70–76
27. Naydenov V, Tosheva L, Antzutkin ON, Sterte J (2005) Meso/macroporous AlPO-5 spherical macrostructures tailored by resin templating. Microporous Mesoporous Mater 78:181–188
28. Zhao X, Wang H, Kang C, Sun Z, Li G, Wang X (2012) Ionothermal synthesis of mesoporous SAPO-5 molecular sieves by microwave heating and using eutectic solvent as structure-directing agent. Microporous Mesoporous Mater 151:501–505
29. Kianfar E, Mahmoud Salimi M (2020) A review on the production of light olefins from hydrocarbons cracking and methanol conversion. In: Advances in chemistry research, vol 59, Nova Science Publishers, Inc., New York
30. Blasco T, Fernandez L, Martinez-Arias A, Sanchez-Sanchez M, Concepcion P, Lopez-Nieto JM (2000) Magnetic resonance studies on V-containing, and V, Mg-containing AFI aluminophosphates. Microporous Mesoporous Mater 39:219–228
31. Machado MS, Perez-Pariente J, Sastre E, Cardoso ED, Giotto MV, García-Fierro J, Fornes V (2002) Characterization and catalytic properties of MAPO-36 and MAPO-5: effect of magnesium content. J Catal 205:299–308
32. Kianfar E (2019) Comparison and assessment of zeolite catalysts performance dimethyl ether and light olefins production through methanol: a review. Rev Inorg Chem 39(3):157–177
33. Álvaro-Muñoz T, Márquez-Álvarez C, Sastre E (2013) Effect of silicon content on the catalytic behavior of chabazite type silicoaluminophosphate in the transformation of methanol to short chain olefins. Catal Today 213:219–225
34. Wang L, Guo C, Yan S, Huang X, Li Q (2003) High-silica SAPO-5 with preferred orientation: synthesis, characterization and catalytic applications. Microporous Mesoporous Mater 64:63–68
35. Weckhuysen M, Rao RR, Martens JA, Schoonheydt RA (1999) Transition metal ions in microporous crystalline aluminophosphates: isomorphous substitution. Eur J Inorg Chem 1999(4):565–577
36. Sankar G, Sánchez-Sánchez M (2018) Metal-substituted microporous aluminophosphates. Springer, New York. https://doi.org/10.1007/430_2018_25
37. Kianfar E (2018) Synthesis and characterization of $AlPO_4$/ZSM-5 catalyst for methanol conversion to dimethylether. Russ J Appl Chem 91(10):1710–1720
38. Kianfar E, Salimi M, Hajimirzaee S, Koohestani B (2018) Methanol to gasoline conversion over CuO/ZSM-5 catalyst synthesized using sonochemistry method. Int J Chem React Eng 17(2):20180127
39. Li Z, Martínez Triguero LJ, Yu J, Corma Canós A (2015) Conversion of methanol to olefins: stabilization of nanosized SAPO-34 by hydrothermal treatment. J Catal 329:379–388
40. Zhao YH, Gao TY, Wang YJ, Zhou YJ, Huang GQ (2018) Zinc supported on alkaline activated HZSM-5 for aromatization reaction. React Kinet Mech Catal 125(2):1085–1098
41. Schulz H (2010) "Coking" of zeolites during methanol conversion: basic reactions of the MTO-, MTP- and MTG processes. Catal Today 154:183–194
42. Ji Y, Yang H, Yan W (2017) Strategies to enhance the catalytic performance of ZSM-5 zeolite in hydrocarbon cracking: a review. Catalysts 7(367):1–31
43. Kianfar E (2019) Nanozeolites: synthesized, properties, applications. J Sol-Gel Sci Tech 91:415–429
44. Sinha AK, Sainkar S, Sivasanker S (1999) An improved method for the synthesis of the silicoaluminophosphate molecular sieves,

Journal : Large 11244 | Article No : 1266 | Pages : 14 | MS Code : 1266 | Dispatch : 20-4-2020

SAPO-5, SAPO-11 and SAPO-31. Microporous Mesoporous Mater 31:321–331
45. Terasaka K, Imai H, Li X (2015) Control of Morphology and acidity of SAPO-5 for the methanol-to- olefins (MTO) reaction. J Adv Chem Eng 5(4):1000138
46. Pinilla-Herrero I, Olsbye U, Márquez-Álvarez C, Sastre E (2017) Effect of framework topology of SAPO catalysts on selectivity and deactivation profile in the methanol-to-olefins reaction. J Catal 352:191–207
47. Westgård-Erichsen M, Svelle S, Olsbye U (2013) H-SAPO-5 as methanol-to-olefins (MTO) model catalyst: towards elucidating the effects of acid strength. J Catal 298:94–101
48. Akolekar DB, Bhargava S (1997) Investigations on the aqueous solution and solid-state cation exchanged MAPO-ATS type molecular sieve. J Mol Catal A 122(1):81–90

Journal : **Large 11244**	Article No : **1266**	Pages : **14**	MS Code : **1266**	Dispatch : **20-4-2020**

Journal:	**11244**
Article:	**1266**

Author Query Form

Please ensure you fill out your response to the queries raised below and return this form along with your corrections

Dear Author

During the process of typesetting your article, the following queries have arisen. Please check your typeset proof carefully against the queries listed below and mark the necessary changes either directly on the proof/online grid or in the 'Author's response' area provided below

Author Proof

Query	Details Required	Author's Response
AQ1	Please confirm if the author names are presented accurately and in the correct sequence (given name, middle name/initial, family name). Author 1 Given name: [Misael García] Last name [Ruiz], Author 2 Given name: [Dora A. Solís] Last name [Casados], Author 3 Given name: [Julia Aguilar] Last name [Pliego], Author 4 Given name: [Carlos Márquez] Last name [Álvarez], Author 5 Given name: [Enrique Sastre de] Last name [Andrés], Author 6 Given name: [Diana Sanjurjo] Last name [Tartalo], Author 7 Given name: [Marisol Grande] Last name [Casas]. Also, kindly confirm the details in the metadata are correct.	
AQ2	Please check and confirm the inserted city in affiliation 2.	
AQ3	As References [2] and [5] are same, we have deleted the duplicate reference and renumbered accordingly. Please check and confirm.	